IEEE Access
Multidisciplinary | Rapid Review | Open Access Journal

Received December 21, 2019, accepted January 6, 2020, date of publication January 8, 2020, date of current version January 17, 2020.

Digital Object Identifier 10.1109/ACCESS.2020.2964902

Isolation Enhancement of Closely Packed Dual Circularly Polarized MIMO Antenna Using Hybrid Technique

MUHAMMAD YASIR JAMAL, (Student Member, IEEE), MIN LI, (Member, IEEE), AND KWAN LAWRENCE YEUNG, (Senior Member, IEEE)
Electrical and Electronic Engineering Department, The University of Hong Kong, Hong Kong

Corresponding author: Min Li (minli@eee.hku.hk)

This work was supported by The University of Hong Kong.

ABSTRACT Mutual coupling always seriously degrades the antenna performance in multiple-input multiple-output (MIMO) systems but this issue has been rarely investigated for antennas with circular polarization. In this paper, a planar and compact circularly polarized MIMO patch antenna with the polarization diversity is presented. Three grounded stubs and a mirrored F-shaped defected ground structure are used to achieve simultaneous matching and isolation between the two patches with offset feeding for circular polarization. The antenna elements are closely packed with the edge-to-edge distance of $0.06\lambda_0$ at the desired frequency of 2.5 GHz. The measured results indicate that the proposed antenna achieves the impedance matching ($S_{11} < -10$ dB), high isolation ($S_{12} < -20$ dB), and circular polarization (axial ratio$<$3 dB) within the frequency band of 2.5-2.55 GHz. The radiation patterns and realized gains are measured, showing good agreement between the simulation and measurement.

INDEX TERMS Circular polarization (CP), multiple-input multiple-output (MIMO), axial ratio (AR), defected ground slot (DGS), envelope correlation coefficient (ECC), left-hand circular polarization (LHCP), right-hand circular polarization (RHCP).

I. INTRODUCTION

Recently, the multiple-input multiple-output (MIMO) technology has become popular due to the increased link capacity especially in complex multipath environments [1]. Various modern wireless applications like long-term evolution (LTE) and Wi-Fi (IEEE 802.11ac, 802.11n) systems are adopting MIMO technology [2]. Circularly polarized (CP) antennas make transmitter and receiver independent of their orientation hence, polarization mismatch losses can be effectively reduced [3].

The superiority of a CP MIMO antenna system over linearly polarized (LP) MIMO system has been extensively studied in [4]. Both multipath (broadcast) and line of sight (LOS, point to point) cases have been investigated by comparing their diversity gain, envelope correlation coefficient, and channel capacity.

From a practical point of view, the multiple antennas in MIMO systems should be closely spaced for compactness. Nevertheless, the closely packed antennas could be strongly coupled to each other due to increased radiation interaction. Numerous techniques have been explored to reduce mutual coupling such as the defected ground structure (DGS) [5], [6], electromagnetic band gap (EBG) structure [7], [8], microstrip stubs [9], shorting pins [10], and parasitic elements [11], [12], etc. These techniques are mostly reported to reduce mutual coupling of LP antennas but the impact of these techniques on the axial ratio (AR) of the CP antenna has been rarely discussed. Certainly, some CP MIMO antennas have been reported for high gain [13], [14], wideband [15]–[17] and planar [18]–[20] applications. Similar decoupling techniques are adopted, such as power dividers [13], DGS [14], and parasitic elements [16], [17]. However, designs in [13], [19] suffered from the complex feeding networks for circular polarization at the expense of occupying a large area. The wideband CP MIMO antennas reported in [16], [17] required simpler feeding structures but incorporated with a very large edge-to-edge spacing of over 0.3λ, making them less appealing for compact applications. The CP MIMO antenna in [20] adopted the coaxial feeding structure to achieve a relatively

The associate editor coordinating the review of this manuscript and approving it for publication was Hayder Al-Hraishawi.

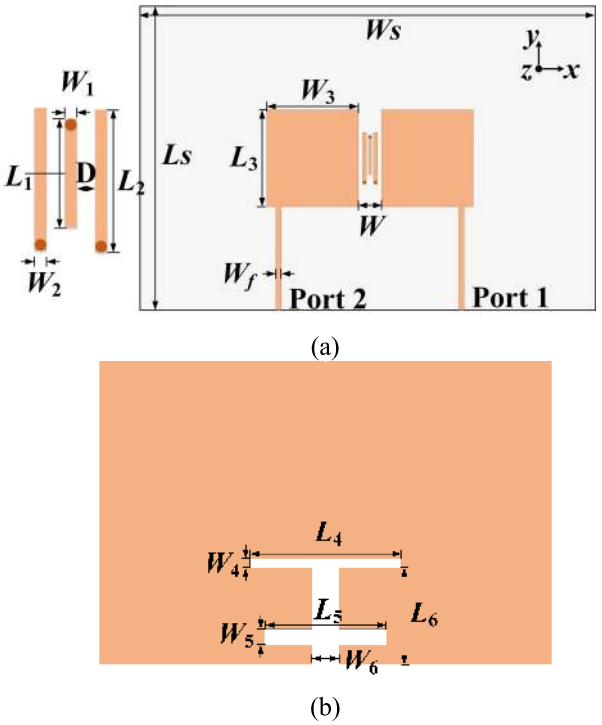

FIGURE 1. Proposed antenna geometry and parameters definition: (a) Top side with grounded stubs and (b) bottom side.

narrow AR bandwidth (ARBW) of 1.5%. In [14], dielectric slabs with simple feeding structures were used to realize the CP MIMO antenna with polarization diversity. However, the 3D construction might not be used for planar applications. A patch antenna was analyzed and designed for CP operation by using the offset feeding structure [21], but it is only for the single-input single-output application. Therefore, the above discussion indicates that the realization of planar CP MIMO antenna with small edge-to-edge separation and simple feeding structure is still a challenge.

In this paper, a planar and compact CP MIMO antenna is presented. Three grounded stubs and a mirrored F-shaped DGS are employed for high isolation and the simple offset feeding is adopted for circular polarization. Meanwhile the desired polarization diversity is also obtained for the MIMO antenna. The idea is benchmarked through fabrication and experiments. Measurement results show that the ARBW of around 2.2% can be achieved.

II. ANTENNA ANALYSIS AND DESIGN

The configuration of the proposed CP MIMO antenna is shown in Fig. 1. The top layer consists of two closely packed rectangular patch antennas with three ground-shorted stubs in between them. The bottom layer is the ground plane with a mirrored F-shaped DGS. The patches are fed with 50 ohms microstrip line with a width of 1.8 mm on a 150 mm × 100 mm ($Ws \times Ls$) Rogers substrate, RO4350B, with the dielectric constant $\varepsilon_r = 3.66$, loss tangent of 0.0037 and the thickness $h = 0.8$ mm. The dimensional parameters are given by: $L_1 = 12.903$, $L_2 = 16.951$, $L_3 = 31.878$, $L_4 = 50$, $L_5 = 40$, $L_6 = 32$, $W_1 = 0.9614$, $W_2 = 1.2626$, $W_3 = 30.355$, $W_4 = 3$, $W_5 = 5.25$, $W_6 = 9$, $W_s = 150$, $L_s = 100$, $W = 7.65$, $D = 0.71$, $W_f = 1.8$, $L_f = 34.06$, $R_{via} = 0.506$. All units are mm. The discussion about the antenna design is divided into two parts in the following subsections *A* and *B*. The first section studies the design of patch antenna with offset feeding for CP radiation, and second section explores the isolation techniques.

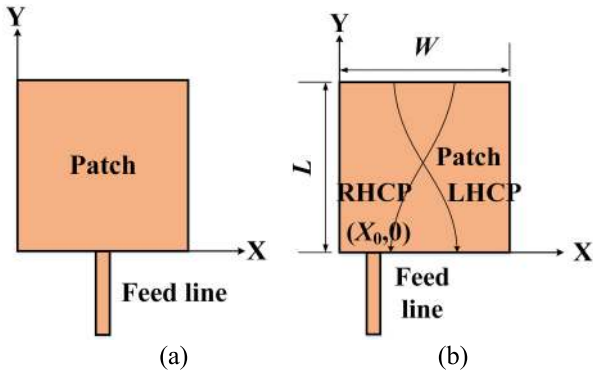

FIGURE 2. (a) Conventional feeding for linear polarized patch antenna. (b) Regions of offset feeding for RHCP and LHCP.

A. PATCH DESIGN WITH OFFSET FEEDING

A rectangular patch antenna is shown in Fig. 2(b), where L is slightly larger than W. It is fed by a microstrip line at a distance X_0 from one of its corners, which is different from the conventional feeding for linear polarization shown in Fig 2(a). The coordinate of the feeding position is (X_0, Y_0), where Y_0 is equal to 0 in this case due to microstrip feeding, while Y_0 can have a positive value for coaxial feeding. According to [21], the TM_{01} and TM_{10} modes are simultaneously excited to generate two orthogonal electric-field (E-field) components in the far field. The two components should have the same magnitude but 90° phase difference for CP radiation, i.e., (1).

$$\frac{E_y}{Ex} = A\frac{\left(k_r - \frac{jk_r}{2Q} - \frac{\pi}{W}\right)}{\left(k_r - \frac{jk_r}{2Q} - \frac{\pi}{L}\right)} = \pm j \tag{1}$$

Rearranging (1) yields

$$\frac{Ak_r}{2Q} - k_r + \frac{\pi}{L} = 0 \tag{2a}$$

$$\frac{k_r}{2Q} + Ak_r - A\frac{\pi}{W} = 0 \tag{2b}$$

where $A = \frac{\cos(\frac{\pi y_0}{L})}{\cos(\frac{\pi x_0}{W})}$, $k_r = k_0\sqrt{\varepsilon_{eff}}$, $k_0 = \frac{2\pi f}{c}$

Thus, Eqns. (1) and (2) can be used to instruct the design parameters of the patch antenna for CP radiation if the feeding position X_0 ($Y_0 = 0$ due to microstrip feeding) and Q-factor is determined. Q for the square patch can be calculated as $Q = 73.7$ using (3) [22] or the simulation method [26]. And the

value of k_r is 95.697 for this case.

$$\frac{1}{Q} = \frac{1}{Q_r} + \frac{1}{Q_c} + \frac{1}{Q_d} \tag{3}$$

In this design, $X_0 = 4$ mm and $Y_0 = 0$ are selected to get $A = 1.096$. Then, $L = 33.1$ mm and $W = 32.6$ mm can be calculated using (1) and (2) at the design frequency $f = 2.5$ GHz. After optimization, the final dimensions of the patch are $L_3 = 31.88$ mm and $W_3 = 30.35$ mm, which are close to those of the calculated values.

Notably, Fig. 2(b) also shows the regions of offset feeding for LHCP and RHCP. According to [21], a quarter-wave transformer is always required for impedance matching of the antenna to 50 Ohms microstrip line, whose need is removed in the proposed design by using the grounded stubs and DGS for simultaneous matching and isolation. Details are discussed in the next section.

B. IMPEDANCE MATCHING AND ISOLATION

The two oppositely fed antennas are placed close to each other with the separation distance $W = 7.65$ mm ($0.06\lambda_0$ at 2.5 GHz). Two isolation techniques have been employed to decrease the mutual coupling and improve the impedance matching and AR bandwidth.

1) STUDY OF THE DGS

The DGS with its specific shape has a significant influence on antenna performance. Fig. 3 shows the impact of different slot configurations on the isolation and matching performances without grounded stubs. It can be seen from Figs. 3(b) and 3(c) that without the DGS, the isolation and matching are both poor. With the insertion of slots gradually, the isolation and matching accordingly improved. But the AR performance still does not meet the 3-dB requirement at 2.5 GHz, as shown in Fig. 3(d). The dimensions of the slots are optimized to achieve the best impedance and isolation.

Besides, it can be seen from Fig. 3(b) that the matching frequency shifts from around 2.45 GHz to 2.5 GHz after added the DGS. And the isolation is accordingly improved from around -10 dB to -25 dB, as shown in Fig. 3(c). It is reasonable that the impedance matching (S_{11}) of a two-element MIMO antenna changed when the isolation level (Z_{21}) is changed, i.e.,

$$S_{11} = \frac{(Z_{11} - Z_0)(Z_{22} + Z_0) - Z_{12}Z_{21}}{(Z_{11} + Z_0)(Z_{22} + Z_0) - Z_{12}Z_{21}}$$

2) STUDY OF THE GROUNDED STUBS

In order to further improve the isolation and AR performances, three grounded stubs are introduced in between the patches. The initial lengths of stubs can be roughly chosen as a quarter wavelength and optimized according to (4) and (5) [12].

$$L_1 = a\frac{\lambda_g}{4} \tag{4}$$

$$L_2 = b\frac{\lambda_g}{4} \tag{5}$$

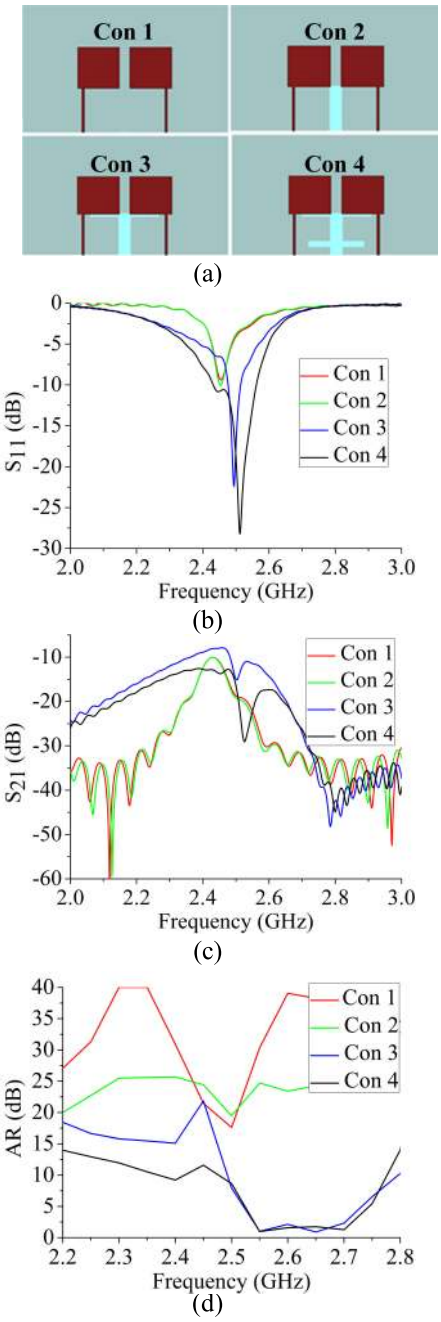

FIGURE 3. (a) Four different antenna configurations. Effect of different slot configurations on (b) S11 (c) S21 and (d) AR.

where

$$\lambda_g = \frac{\lambda_0}{\sqrt{\varepsilon_{eff}}}$$

$$\varepsilon_{eff} = \frac{\varepsilon_r + 1}{2} + \frac{\varepsilon_r - 1}{2\sqrt{(1 + 12\frac{h}{w})}} \quad \text{for } \frac{w}{h} > 1$$

a and b are the correction factors due to proximity effects, and λ_g is the guided wavelength in the dielectric between stubs and ground. Based on the above design formulas, the stubs can be designed for any frequency and substrate.

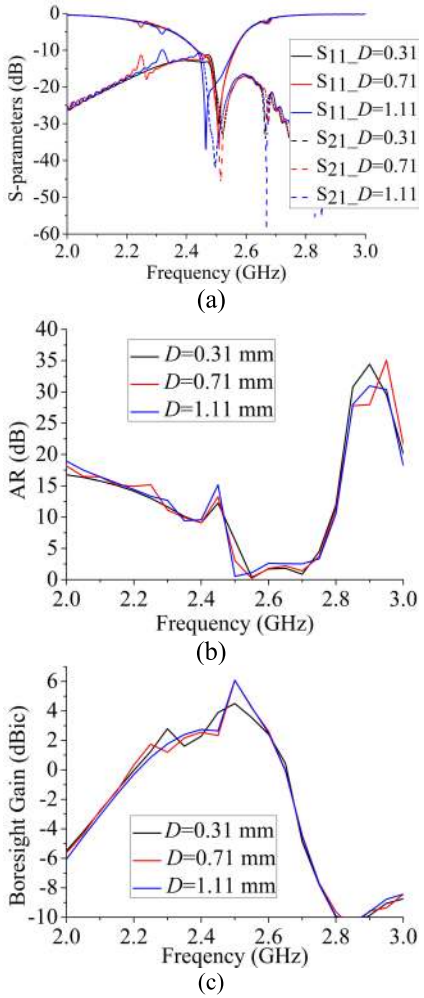

FIGURE 4. Effect of D on (a) S-Parameters (b) AR and (C) boresight gain.

In this design, λ_g is calculated as 71.97 mm, and the optimum values of a and b are 0.72 and 0.94, respectively.

Fig. 4 shows the effect of the gap D between the grounded stubs on impedance matching, AR and boresight gain while keeping the antenna spacing as $W = 7.65$ mm. It can be seen that when $D = 0.71$ mm, the isolated impedance bandwidth with $S_{11} \leq$-10 dB and $S_{21} \leq$-20 dB ranges from 2.47-2.55 GHz, which is a little different from that of the 3-dB AR bandwidth of 2.5-2.65 GHz. Moreover, the matching (S_{11}) and isolated (S_{21}) frequencies increase with decreasing the gap D. Hence, the impedance bandwidth and AR bandwidth can be overlapped with decreased D. But the boresight gain drops a lot when D increases, as shown in Fig. 4(c). Hence, in the final design, $D = 0.71$ mm is chosen for achieving a relatively high gain.

Fig 5 shows the effects of the length and width of the ground on the antenna performance. It can be observed that both the length and width of the ground have little impact on the impedance matching, isolation, and AR of the MIMO antenna.

The simulated current distribution in Fig. 6 is further used to demonstrate the decoupling mechanism. It shows that in

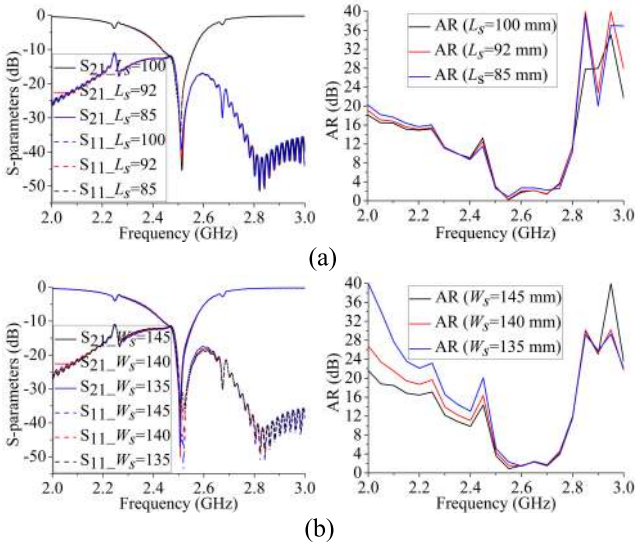

FIGURE 5. Simulated S-parameters and axial ratio for different values of ground: (a) Length. (b) Width.

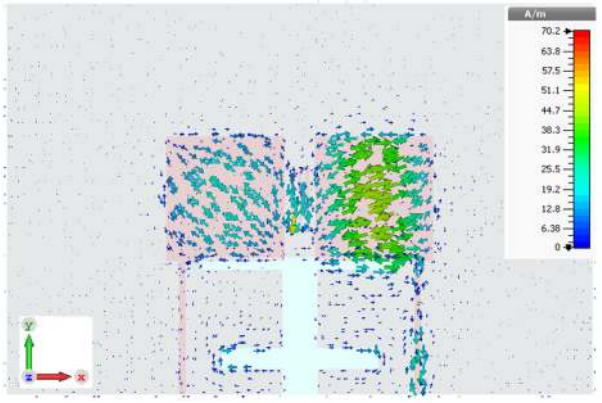

FIGURE 6. Simulated surface-current distributions of the proposed CP MIMO antenna when port 1 is excited.

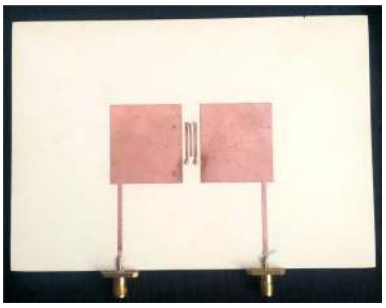

FIGURE 7. The protype of the proposed CP MIMO antenna.

the proposed design when port 1 is excited, both antennas are distributed with strong current distributions. However, the currents on each antenna are orthogonal to each other. As a result, the current arriving at port 2 is very weak, indicating the high port isolation.

III. FABRICATION AND MEASUREMENTS

A prototype of the proposed antenna is shown in Fig. 7. The S-parameters are measured using the vector network

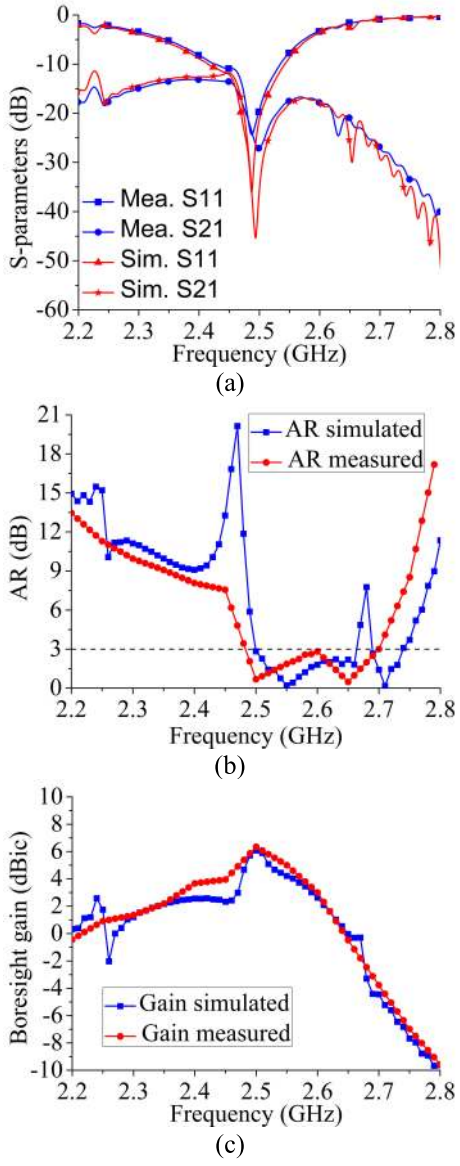

FIGURE 8. Simulated and measured (a) S-parameters, (b) axial ratio (AR) and (c) boresight gain of the proposed antenna.

analyzer (VNA) Rohde & Schwarz ZVA 24 and the radiation pattern is measured using the Satimo Starlab. The simulated and measured scattering parameters, AR & boresight gain, and radiation patterns of the final design are shown in Figs. 8 and 9. It can be seen that the measurement agreed well with the simulation.

Fig. 8(a) shows that the proposed design meets the requirements of impedance matching and isolation within the frequency band of 2.47-2.55 GHz (3.2%) with simulated S_{11} ≤-10 dB and $S_{21} \leq -20$ dB. The simulated 3-dB AR bandwidth is 2.50-2.66 GHz, as shown in Fig. 8(b). Hence, the overlapping isolated impedance bandwidth of the proposed antenna is 2.50-2.55 GHz for CP radiation. Fig. 8(c) shows the simulated and measured realized gains of the antenna in boresight direction (+z-direction). It can be seen that the antenna has a maximum gain

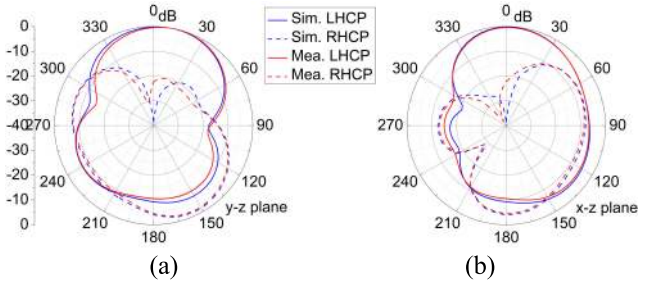

FIGURE 9. The radiation pattern of the proposed antenna in (a) the *y-z* plane (b) the *x-z* plane when port 1 is excited at 2.55 GHz.

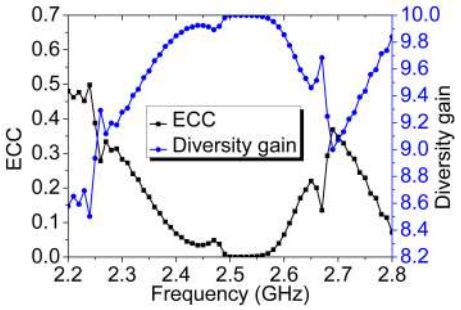

FIGURE 10. ECC and diversity gain versus frequency.

of 6.1 dBi at 2.5 GHz with a slight 1-dBi reduction at 2.55 GHz.

The normalized radiation patterns of the proposed antenna are shown in Fig. 9 when port 1 is excited at 2.55 GHz, where the antenna achieves the lowest simulated AR of around 0.21. Due to the symmetric layout, the patterns for port 2 are not shown to save space. It can be seen that in both the *y-z* plane ($\Phi = 90°$) and *x-z* plane ($\Phi = 0°$), the MIMO antenna performances the boresight radiation directed to the +z-direction. Besides, the radiation of left-hand circular polarization (LHCP) of the antenna is much stronger than that of the right-hand circular polarization (RHCP) in the +z-direction when port 1 is excited, indicating the LHCP radiation for port 1. Similarly, the antenna performs the RHCP radiation for port 2 due to the symmetric layout. Hence, the polarization diversity of the CP MIMO antenna can be achieved.

The envelope correlation coefficient (ECC) i.e.ρ and diversity gain i.e. G are calculated using the far-field vector phasor radiation patterns by (6) and (7), respectively [23]–[25]. The calculated results are shown in Fig. 10. It can be seen that the diversity gain is approximately equal to its theoretical maximum value of around 10 considering selection combining [24]. Besides, the proposed two-port MIMO antenna also meets the criterion for ECC [23], i.e., the ECC is around 0.003 which is much smaller than 0.5 within the desired band of 2.5-2.55 GHz.

$$\rho_e = \frac{\left| \iint_{4\pi} [\vec{E_1}(\theta,\phi) \cdot \vec{E_2}(\theta,\phi)] d\Omega \right|^2}{\iint_{4\pi} \left| \vec{E_1}(\theta,\phi) \right|^2 d\Omega \iint_{4\pi} \left| \vec{E_2}(\theta,\phi) \right|^2 d\Omega} \tag{6}$$

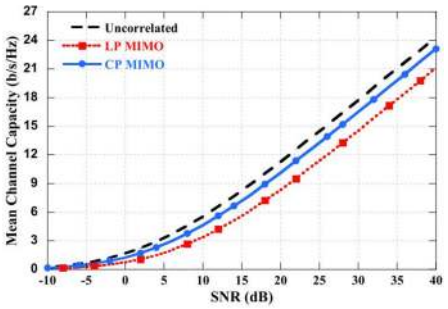

FIGURE 11. Performance enhancement (channel capacity) by using CP MIMO over LP MIMO [4].

where

$$\vec{E_1}(\theta,\phi)\cdot\vec{E_2}(\theta,\phi) = E_{\theta 1}(\theta,\phi)E^*_{\theta 2}(\theta,\phi) + E_{\phi 1}(\theta,\phi)E^*_{\phi 2}(\theta,\phi)$$

$$G = 10\times\sqrt{1-\rho^2} \tag{7}$$

In conclusion, the proposed antenna could achieve the pattern and polarization diversity when different ports are excited. And a very low ECC further ensures the excellent MIMO performance. Thus, the CP antenna could achieve both low AR and high isolation as compared to an LP MIMO antenna, for which the isolation issue is the main concern.

Fig. 11 shows the comparison of performance improvement by using CP MIMO instead of LP MIMO. It can be observed that for a given SNR like 15 dB the channel capacity is increased from around 5.7 b/s/Hz to 7 b/s/Hz by adopting CP MIMO over LP MIMO.

Then, a comparison of the proposed antenna with and without using the DGS & grounded stubs for isolation is conducted in terms of the efficiency, gain and radiation patterns. Fig. 12 shows the simulated comparison results when port 1 is excited. It can be seen from Fig. 12(a) that the maximum efficiency and boresight gain increase from around 56.5% to 91.6% and 4.49 dBi to 6.07 dBi, respectively. The patterns in Figs. 12(b) and (c) indicate that without using the DGS and grounded stubs, the antenna performs the poor CP radiation with comparable radiations of LHCP and RHCP due to the interaction between two antennas. After adopting the decoupling structures, the CP performance is significantly improved with very weak (lower than -30 dB) RHCP radiation (crossed-polarized radiation) in the boresight direction for port 1, indicating the LHCP radiation for port 1.

Table 1 compares the proposed antenna with some related works already studied in the literature. It can be observed that the proposed design could achieve the high isolation for very small element separation distance. The resulted isolated impedance bandwidth of around 3.2% is close to that of a conventional patch antenna of around 1-3%. Besides, the ARBW of around 2.2% in this design is even better as compared to a typical CP patch antenna using the off-center feeding structure [21] and the CP MIMO antenna of 1.5% in [20].

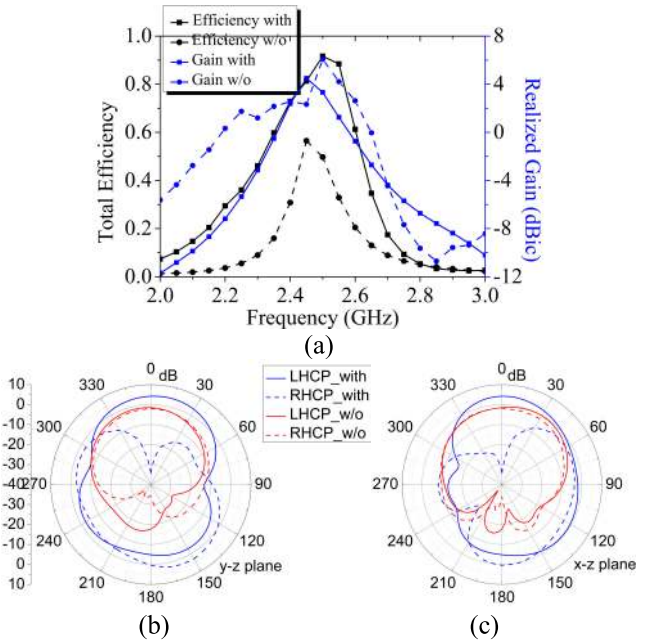

FIGURE 12. The comparison of the proposed antenna with and without using the DGS & grounded stubs for isolation when port 1 is excited: (a) efficiency & gain and (b)&(c) radiation patterns.

TABLE 1. Performance comparison with previous CP MIMO antennas.

Ref	Edge to edge Spacing (λ)	S21 (dB)	ARBW (%)	Isolation Technique	Feeding+ Complexity	Ant. Height (mm)	Max Gain (dBi)
[14]	0.19	-25	4.5	DGS	Microstrip +Simple	7.6	4.7
[16]	0.3	-25	23	PE	Microstrip +Simple	N.G.	4
[17]	0.5	-30	20.8	PE + DRA	Microstrip +Simple	26.1	5.2
[19]	>0.6	-30	<1.2	N.G.	Coaxial +Complex	1.6	15
[20]	N.G.	-15	<1.5	Orthogonal modes	Coaxial +Simple	0.127	N.G.
Proposed	0.06	-20	2.2	Grounded Stubs +DGS	Microstrip +Simple	0.8	6.1

DGS=Defected ground slot, PE=Parasitic element, and DRA=Dielectric resonator antenna.

Furthermore, the proposed antenna could achieve the high gain & front-to-back ratio with a planar configuration.

IV. CONCLUSION

A two-element CP MIMO patch antenna with polarization diversity was presented in this paper. The offset feeding is used for circular polarization. The high isolation is achieved by using the defected ground structure and grounded stubs. The antenna achieved good impedance matching, high isolation, high gain, and polarization diversity simultaneously with a simple planar structure. Compared to the MIMO

antennas found in literature, the proposed antenna requires very small element separation distance and simple feeding structure to realize the ARBW of 2.2% and impedance bandwidth of 3.2%. The antenna is designed for 802.11n 2.5 GHz band for Wi-Fi applications.

ACKNOWLEDGMENT

The authors would like to thank the Department of Electrical and Electronics Engineering, Faculty of Engineering, The University of Hong Kong, for providing material and equipment for this project.

REFERENCES

[1] R. Murch and K. Letaief, "Antenna systems for broadband wireless access," *IEEE Commun. Mag.*, vol. 40, no. 4, pp. 76–83, Apr. 2002.
[2] E. G. Larsson, O. Edfors, F. Tufvesson, and T. L. Marzetta, "Massive MIMO for next generation wireless systems," *IEEE Commun. Mag.*, vol. 52, no. 2, pp. 186–195, Feb. 2014.
[3] Y. Ding and K. Wa Leung, "Dual-band circularly polarized dual-slot antenna with a dielectric cover," *IEEE Trans. Antennas Propag.*, vol. 57, no. 12, pp. 3757–3764, Dec. 2009.
[4] F. A. Dicandia, S. Genovesi, and A. Monorchio, "Analysis of the performance enhancement of MIMO systems employing circular polarization," *IEEE Trans. Antennas Propag.*, vol. 65, no. 9, pp. 4824–4835, Sep. 2017.
[5] A. A. Ibrahim, M. A. Abdalla, A. B. Abdel-Rahman, and H. F. A. Hamed, "Compact MIMO antenna with optimized mutual coupling reduction using DGS," *Int. J. Microw. Wireless Technol.*, vol. 6, no. 2, pp. 173–180, Apr. 2014.
[6] S. Kamal and A. A. Chaudhari, "Printed meander line MIMO antenna integrated with air gap, DGS AND RIS: A low mutual coupling design for LTE applications," *Prog. Electromagn. Res. C*, vol. 71, pp. 149–159, 2017.
[7] F. Yang and Y. Rahmat-Samii, "Microstrip antennas integrated with electromagnetic band-gap (EBG) structures: A low mutual coupling design for array applications," *IEEE Trans. Antennas Propag.*, vol. 51, no. 10, pp. 2936–2946, Oct. 2003.
[8] E. Rajo-Iglesias, O. Quevedo-Teruel, and L. Inclan-Sanchez, "Mutual coupling reduction in patch antenna arrays by using a planar EBG structure and a multilayer dielectric substrate," *IEEE Trans. Antennas Propag.*, vol. 56, no. 6, pp. 1648–1655, Jun. 2008.
[9] L. Liu, S. W. Cheung, and T. I. Yuk, "Compact MIMO antenna for portable devices in UWB applications," *IEEE Trans. Antennas Propag.*, vol. 61, no. 8, pp. 4257–4264, Aug. 2013.
[10] S. Shoaib, I. Shoaib, N. Shoaib, X. Chen, and C. G. Parini, "Design and performance study of a dual-element multiband printed monopole antenna array for MIMO terminals," *IEEE Antennas Wireless Propag. Lett.*, vol. 13, pp. 329–332, 2014.
[11] M. U. Khan and M. S. Sharawi, "A 2×1 multiband MIMO antenna system consisting of miniaturized patch elements," *Microw. Opt. Technol. Lett.*, vol. 56, pp. 1371–1375, Jun. 2014.
[12] R. Zaker, "Design of a very closely-spaced antenna array with a high reduction of mutual coupling using novel parasitic L-shaped strips," *Int. J. RF Microw. Comput. Aided Eng.*, vol. 28, no. 9, Nov. 2018, Art. no. e21422.
[13] S. Karamzadeh, V. Rafiei, and H. Saygin, "PD FPR CP high-gain MIMO antenna," *Electron. Lett.*, vol. 53, no. 17, pp. 1174–1176, 2017.
[14] G. Das, A. Sharma, and R. K. Gangwar, "Dielectric resonator based circularly polarized MIMO antenna with polarization diversity," *Microw. Opt. Technol. Lett.*, vol. 60, no. 3, pp. 685–693, 2018.
[15] Nasimuddin, X. Qing, and Z. N. Chen, "A wideband circularly polarized antenna for low mutual coupling Ka-band phased arrays," in *Proc. IEEE Region 10 Conf. (TENCON)*, Nov. 2016, pp. 1065–1067.
[16] I. Adam, M. N. M. Yasin, N. Ramli, M. Jusoh, H. A. Rahim, T. B. A. Latef, T. F. T. M. N. Izam, and T. Sabapathy, "Mutual coupling reduction of a wideband circularly polarized microstrip MIMO antenna," *IEEE Access*, vol. 7, pp. 97838–97845, 2019.
[17] J. Iqbal, U. Illahi, M. I. Sulaiman, M. M. Alam, M. M. Suud, and M. N. M. Yasin, "Mutual coupling reduction using hybrid technique in wideband circularly polarized MIMO antenna for WiMAX applications," *IEEE Access*, vol. 7, pp. 40951–40958, 2019.
[18] T.-D. Yeo, S. C. Chae, B. Ahn, and J.-W. Yu, "Rotational circularly polarized array antenna for mutual coupling reduction," in *Proc. Int. Symp. Antennas Propag. (ISAP)*, Oct. 2017, pp. 1–2.
[19] M. K. A. Nayan, M. F. Jamlos, and M. A. Jamlos, "Mimo circular polarization array antenna with dual coupled 90° phased shift for point-to-point application," *Microw. Opt. Technol. Lett.*, vol. 57, no. 4, pp. 809–814, Apr. 2015.
[20] Z. Yang and K. F. Warnick, "Analysis and design of intrinsically dual circular polarized microstrip antennas using an equivalent circuit model and jones matrix formulation," *IEEE Trans. Antennas Propag.*, vol. 64, no. 9, pp. 3858–3868, Sep. 2016.
[21] S. K. Lee, A. Sambell, E. Korolkiewicz, and S. F. Ooi, "Analysis and design of a circular-polarized nearly-square-patch antenna using a cavity model," *Microw. Opt. Technol. Lett.*, vol. 46, no. 4, pp. 406–410, Aug. 2005.
[22] E. G. Lim, "Circular polarised microstrip antenna design using segmental methods," Ph.D. dissertation, Univ. Northumbria, Newcastle, U.K., 2002.
[23] R. G. Vaughan and J. B. Andersen, "Antenna diversity in mobile communications," *IEEE Trans. Veh. Technol.*, vol. VT-36, no. 4, pp. 147–172, Nov. 1987.
[24] J. Yang, S. Pivnenko, T. Laitinen, J. Carlsson, and X. Chen, "Measurement of diversity gain and radiation efficiency of the eleven antenna by using different measurement techniques," in *Proc. 5th Eur. Conf. Antennas Propag.*, 2010, pp. 1–5.
[25] T. Taga, "Analysis for mean effective gain of mobile antennas in land mobile radio environments," *IEEE Trans. Veh. Technol.*, vol. 39, no. 2, pp. 117–131, May 1990.
[26] *Ansoft Ensemble V8*, Ansoft Corp., Pittsburgh, PA, USA, 2001.
[27] C. Balanis, *Antenna Theory: Analysis and Design*, 3rd ed. Hoboken, NJ, USA: Wiley, 2005.

MUHAMMAD YASIR JAMAL was born in Bahawalnagar, Pakistan, in 1986. He received the B.Sc. and M.Sc. degrees in electronics and communication engineering from the University of Engineering and Technology at Lahore, Lahore, Pakistan, in 2009 and 2015, respectively. He is currently pursuing the Ph.D. degree with the Department of Electrical and Electronic Engineering, The University of Hong Kong, Hong Kong. He was a Lecturer with the University of Engineering and Technology at Lahore. His research interests include antennas, waveguides and radio propagation, and RF and microwaves technology.

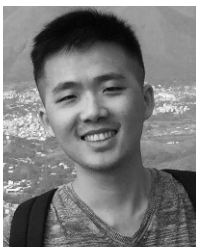

MIN LI (Member, IEEE) received the B.S. degree from UESTC, Chengdu, China, in 2014, and the Ph.D. degree from The University of Hong Kong, Hong Kong, in 2018. He is currently a Postdoctoral Researcher with the Department of Electrical and Electronic Engineering, The University of Hong Kong. His current research interests include antenna design and multiple-input multiple-output antenna decoupling.

KWAN LAWRENCE YEUNG (Senior Member, IEEE) was born in 1969. He received the B.Eng. and Ph.D. degrees in information engineering from The Chinese University of Hong Kong, in 1992 and 1995, respectively. He joined the Department of Electrical and Electronic Engineering, The University of Hong Kong, in July 2000, where he is currently a Professor. His research interests include the next-generation Internet, packet switch/router design, all-optical networks, and wireless data networks.